Electronic Supplementary Material (ESI) for Journal of Materials Chemistry C.
This journal is © The Royal Society of Chemistry 2024

Supporting Information

Explorations of Highly Birefringent Materials in the Vanadium Oxyfluoride–Iodate System by Fluoride Ion Modulation

Yu Huang [1,2], Xue-Ying Zhang [1], San-Gen Zhao[1], Jiang-Gao Mao[1,3], and Bing-Ping Yang [1,3]*

[1] State Key Laboratory of Structural Chemistry, Fujian Institute of Research on the Structure of Matter, Chinese Academy of Sciences, Fuzhou, 350002, Fujian

[2] State Key Laboratory of Material Processing and Die & Mould Technology, School of Materials Science and Engineering, Huazhong University of Science and Technology, Wuhan, 430074, Hubei

[3] University of Chinese Academy of Sciences, Beijing, 100049

*Corresponding Author: Bing-Ping Yang: ybp@fjirsm.ac.cn

Table of contents

Table S1. Crystallographic data for $Sr[VO_2F(IO_3)_2]$ and $Sr_3F_2(VO_2F_4)(IO_3)$.

Formula	$Sr[VO_2F(IO_3)_2]$	$Sr_3F_2(VO_2F_4)(IO_3)$
Formula weight	539.36	634.70
T (K)	294(8)	295.15(10)
Crystal system	Orthorhombic	Monoclinic
Space group	*Pbcn*	*C*2/*c*
a (Å)	5.1454(10)	20.681(4)
b (Å)	12.272(2)	5.4749(7)
c (Å)	12.1220(18)	16.686(3)
α (°)	90	90
β (°)	90	100.362(16)
γ (°)	90	90
V (Å^3)	765.5(2)	1858.5(5)
Z	4	8
ρ_{calc} (g/cm^3)	4.680	4.537
μ (mm^{-1})	16.289	21.523
F(000)	960.0	2272.0
R_{int}	0.0522	0.0447
Goodness-of-fit on F^2	1.098	0.982
R_1, wR_2 [I>=2σ (I)]	0.0401/0.0927	0.0500/0.1002
R_1, wR_2 [all data]	0.0571/0.1058	0.0836/0.1200

$R_1 = \sum||F_o|-|F_c||/\sum|F_o|$; $wR_2 = [\sum w(F_o^2-F_c^2)^2]/\sum w(F_o^2)^2]^{1/2}$

Table S2. Selected bond lengths (Å) and angles (°) for $Sr[VO_2F(IO_3)_2]$

I(1)−O(1)	1.799(8)	Sr(1)−O(2)#2	2.812(7)
I(1)−O(2)	1.800(7)	Sr(1)−O(2)#4	2.812(7)
I(1)−O(3)	1.850(7)	Sr(1)−O(1)	2.602(8)
Sr(1)−F(1)#3	2.711(3)	Sr(1)−O(1)#6	2.602(8)
Sr(1)−F(1)#1	2.711(3)	V(1)−F(1)	1.907(9)
Sr(1)−O(4)#4	2.694(7)	V(1)−O(4)	1.621(7)
Sr(1)−O(4)#2	2.694(7)	V(1)−O(4)#7	1.621(7)
Sr(1)−O(3)#5	2.819(7)	V(1)−O(3)#7	1.968(7)
Sr(1)−O(3)#3	2.819(7)	V(1)−O(3)	1.968(7)
O(2)−I(1)−O(3)	98.2(3)	O(4)#9−V(1)−O(4)	103.7(5)
O(1)−I(1)−O(3)	97.2(4)	O(4)−V(1)−O(3)#9	99.3(3)
O(1)−I(1)−O(2)	101.2(4)	O(4)#9−V(1)−O(3)	99.3(3)
F(1)−V(1)−O(3)#9	77.3(2)	O(4)#9−V(1)−O(3)#9	96.3(3)
F(1)−V(1)−O(3)	77.3(2)	O(4)−V(1)−O(3)	96.3(3)
O(4)−V(1)−F(1)	128.1(3)	O(3)#9−V(1)−O(3)	154.6(4)
O(4)#9−V(1)−F(1)	128.1(3)		

Symmetry transformations used to generate equivalent atoms: #1 1-x, 1-y, 1-z; #2 3/2-x, 3/2-y, 1/2+z; #3 1/2-x, 3/2-y, 1/2+z; #4 1/2+x, 3/2-y, 1-z; #5 +x, 1-y, 1/2+z; #6 1-x, +y, 3/2-z; #7 1/2-x, 3/2-y, -1/2+z; #9 1-x, +y, 1/2-z

Table S3. Selected bond lengths (Å) and angles (°) for $Sr_3F_2(VO_2F_4)(IO_3)$.

I(1)−O(1)	1.804(6)	Sr(2)−F(5)#3	2.876(6)
I(1)−O(2)	1.798(6)	Sr(2)−O(3)#6	2.666(7)
I(1)−O(3)	1.794(7)	Sr(2)−O(4)#7	2.882(8)
Sr(1)−F(1)	2.457(6)	Sr(3)−F(1)#6	2.477(5)
Sr(1)−F(2)	2.460(6)	Sr(3)−F(1)#4	2.484(6)
Sr(1)−F(5)#3	2.573(5)	Sr(3)−F(2)#4	2.481(5)
Sr(1)−F(6)#4	2.506(6)	Sr(3)−F(2)	2.464(5)
Sr(1)−O(1)	2.581(8)	Sr(3)−F(3)#4	2.503(5)
Sr(1)−O(1)#1	2.598(7)	Sr(3)−F(4)#8	2.503(5)
Sr(1)−O(2)#5	2.637(6)	Sr(3)−F(6)#4	2.622(6)
Sr(1)−O(3)#6	2.620(7)	Sr(3)−O(2)#1	2.735(7)
Sr(2)−F(1)#6	2.561(5)	V(1)−F(3)	2.177(6)
Sr(2)−F(2)	2.499(5)	V(1)−F(4)	2.031(6)
Sr(2)−F(3)#7	2.488(5)	V(1)−F(5)	1.908(6)
Sr(2)−F(3)	2.425(6)	V(1)−F(6)	1.898(5)
Sr(2)−F(4)	2.631(6)	V(1)−O(4)	1.692(6)
Sr(2)−F(4)#3	2.656(5)	V(1)−O(5)	1.603(8)
Sr(2)−F(5)#7	2.824(5)	O(2)−I(1)−O(1)	99.1(3)
O(3)−I(1)−O(1)	97.6(3)	O(4)−V(1)−F(5)	91.4(3)
F(5)−V(1)−F(4)	82.2(2)	O(4)−V(1)−F(6)	95.7(3)
F(6)−V(1)−F(3)	78.4(2)	O(5)−V(1)−F(3)	173.1(3)
F(6)−V(1)−F(4)	83.7(3)	O(5)−V(1)−F(4)	95.0(3)
F(6)−V(1)−F(5)	156.6(3)	O(5)−V(1)−F(5)	99.8(3)
O(4)−V(1)−F(3)	82.2(3)	O(5)−V(1)−F(6)	100.0(3)
O(4)−V(1)−F(4)	160.1(3)	O(5)−V(1)−O(4)	104.7(4)
O(3)−I(1)−O(2)	104.3(3)		

Symmetry transformations used to generate equivalent atoms: #1 1-x, 1-y, 1-z; 2+x, -1+y, +z; #3 3/2-x, -1/2+y, 3/2-z; #4 3/2-x, 3/2-y, 1-z; #5 1-x, -y, 1-z; #6 +x, 1+y, +z; #7 3/2-x, 1/2+y, 3/2-z; #8 3/2-x, 5/2-y, 1-z

Table S4. Calculated dipole moments of IO_3 and VO_4F units, and the net dipole moment of a unit cell for $Sr[VO_2F(IO_3)_2]$.

$Sr[VO_2F(IO_3)_2]$ (Z = 4)				
Species	Dipole moment (D = Debye)			
	x(a)	y(b)	z(c)	Total magnitude
$I1(1)O_3$	13.443	−2.180	−4.263	14.271
$I2(1)O_3$	−13.443	−2.180	4.263	14.271
$I1(2)O_3$	−13.443	−2.180	−4.263	14.271
$I2(2)O_3$	13.443	−2.180	4.263	14.271
$I1(3)O_3$	−13.443	2.180	−4.263	14.271
$I2(3)O_3$	13.443	2.180	4.263	14.271
$I1(4)O_3$	13.443	2.180	−4.263	14.271
$I2(4)O_3$	−13.443	2.180	4.263	14.271
$V(1)O_4F$	0	0.178	0	0.178
$V(2)O_4F$	0	0.178	0	0.178
$V(3)O_4F$	0	−0.178	0	0.178
$V(4)O_4F$	0	−0.178	0	0.178

Table S5. Calculated dipole moments of IO_3 and VO_2F_4 units, and the net dipole moment of a unit cell for $Sr_3F_2(VO_2F_4)(IO_3)$.

$Sr_3F_2(VO_2F_4)(IO_3)$ (Z = 8)				
Species	Dipole moment (D = Debye)			
	x(a)	y(b)	z(c)	Total magnitude
$I(1)O_3$	3.108	−0.431	−13.826	14.178
$I(2)O_3$	−3.108	−0.431	13.826	14.178
$I(3)O_3$	3.108	0.431	−13.826	14.178
$I(4)O_3$	−3.108	0.431	13.826	14.177
$I(5)O_3$	3.108	−0.431	−13.826	14.178
$I(6)O_3$	−3.108	−0.431	13.826	14.178
$I(7)O_3$	3.108	0.431	−13.826	14.178
$I(8)O_3$	−3.108	0.431	13.826	14.178
$V(1)O_2F_4$	9.256	2.645	1.298	9.714
$V(2)O_2F_4$	9.256	−2.645	1.298	9.714
$V(3)O_2F_4$	−9.256	2.645	−1.298	9.714
$V(4)O_2F_4$	−9.256	−2.645	−1.298	9.714
$V(5)O_2F_4$	9.256	2.645	1.298	9.714
$V(6)O_2F_4$	9.256	−2.645	1.298	9.714
$V(7)O_2F_4$	−9.256	2.645	−1.298	9.714
$V(8)O_2F_4$	−9.256	−2.645	−1.298	9.714

Table S6. Comparison of some birefringent materials.

compound	birefringence
TiO_2[1, 2]	0.256 at 546 nm ^{exp}
α-BaB_2O_4[3]	0.122 at 532 nm ^{exp}
MgF_2[4, 5]	0.012 at 546 nm ^{exp}
$LiNbO_3$[6-9]	0.074 at 1300 nm ^{exp}
YVO_4[10]	0.204 at 532 nm ^{exp}
$CaCO_3$[11, 12]	0.172 at 532 nm ^{exp}
$NaVO_2(IO_3)_2(H_2O)$[13]	0.150 at 1064 nm ^{cal}
$K_3V_2O_3F_4(IO_3)_3$[14]	0.158 at 2050 nm ^{cal}
$CsVO_2F(IO_3)$[15]	0.040 at 2050 nm ^{cal}
$Cs_2VOF_4(IO_2F_2)$[16]	0.088 at 1064 nm ^{cal}
α-$Ba_2[VO_2F_2(IO_3)_2]IO_3$[17]	0.200 at 2050 nm ^{cal}
$Zn_2(VO_4)(IO_3)$[18]	0.180 at 1064 nm ^{cal}
$CsZrF_4(IO_3)$[19]	0.200 at 1064 nm ^{cal}
$LiMoO_3(IO_3)$[20, 21]	0.178 at 1064 nm ^{cal}
$NaMoO_3(IO_3)$[21]	0.208 at 1064 nm ^{cal}
$KRb[(MoO_3)_2(IO_3)_2]$[22]	0.146 at 1064 nm ^{cal}
γ-$KMoO_3(IO_3)$[21]	0.087 at 1064 nm ^{cal}
$RbMoO_2F_3(IO_2F_2)$[23]	0.217 at 1064 nm ^{cal}
$CsMoO_2F_3(IO_2F_2)$[23]	0.203 at 1064 nm ^{cal}
$Ba_2[MoO_3F(IO_3)](MoO_3F_2)$[24]	0.264 at 532 nm ^{cal}
$Ba_2[MoO_3(OH)(IO_3)_2]IO_3$[25]	0.225 at 1064 nm ^{cal}
$Sc(IO_3)_2(NO_3)$[26]	0.348 at 546 nm ^{exp}
$CeF_2(SO_4)$[27]	0.360 at 546 nm ^{exp}
α-$Ba_2[GaF_4(IO_3)_2](IO_3)$[28]	0.126 at 1064 nm ^{cal}
β-$Ba_2[GaF_4(IO_3)_2](IO_3)$[28]	0.135 at 1064 nm ^{cal}
$Ba_2[FeF_4(IO_3)_2]IO_3$[29]	0.125 at 1064 nm ^{cal}
$Ba[FeF_4(IO_3)]$[29]	0.053 at 1064 nm ^{cal}
$Zn(IO_3)F$[30]	0.194 at 1064 nm ^{cal}

$Cd(IO_3)F$[31]	0.072 at 1064 nm [cal]
$Y(IO_3)_2F$[32]	0.041 at 1064 nm [cal]
$HfF_2(IO_3)_2$[33]	0.333 at 550 nm [cal]
$LiGaF_2(IO_3)_2$[34]	0.181 at 1064 nm [cal]
$Ba(IO_3)F$[35]	0.1253 at 589.3 nm [cal]
$CeF_2(IO_3)_2$[36]	0.14 at 1064 nm [cal]
$CeF_2(IO_3)_2(H_2O)$[37]	0.046 at 1064 nm [cal]
$(NH_4)Bi_2(IO_3)_2F_5$[38]	0.069 at 589.3 nm [cal]
$Ce(IO_3)_3F$[39]	0.225 at 546 nm [cal]
$NaGa(IO_3)_2F_2$[40]	0.21 at 1064 nm [cal]
$CsHfF_4(IO_3)$[41]	0.161 at 532 nm [cal]
$Ba[InF_3(IO_3)_2]$[42]	0.172 at 1064 nm [cal]
$PbFIO_3$[43]	0.07 at 546.1nm [cal]
$RbGaF_3(IO_3)$[44]	0.174 at 1064 nm [cal]
$ZrF_2(IO_3)_2$[44]	0.329 at 1064 nm [cal]
$Li_2Ce(IO_3)_4F_2$[45]	0.054 at 589 nm [cal]
$Cd_3(IO_3)(IO_4)F_2 \cdot 0.1CdO$[46]	0.133 at 546.1 nm [cal]
$Sr[VO_2F(IO_3)_2]$	**0.250 at 550 nm [cal]**
$Sr_3F_2(VO_2F_4)(IO_3)$	**0.406 at 550 nm [cal]**

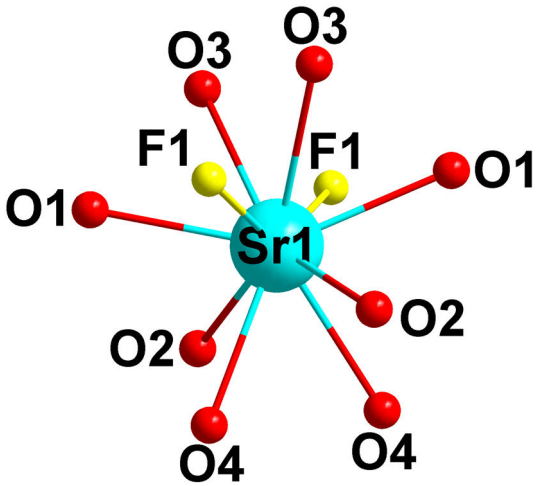

Figure S1. Coordination environment of the Sr^{2+} cation for $Sr[VO_2F(IO_3)_2]$.

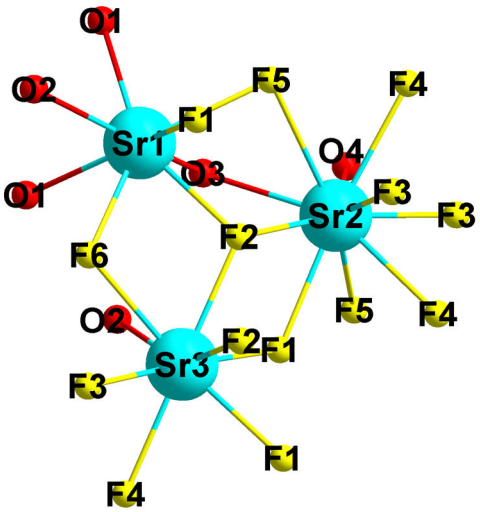

Figure S2. Coordination environments of Sr^{2+} cations for $Sr_3F_2(VO_2F_4)(IO_3)$.

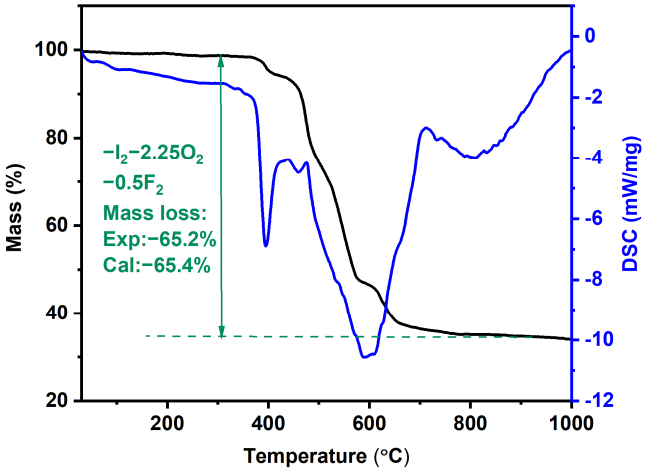

Figure S3. Thermogravimetric analysis and differential scanning calorimetry curves of $Sr[VO_2F(IO_3)_2]$ under a N_2 atmosphere.

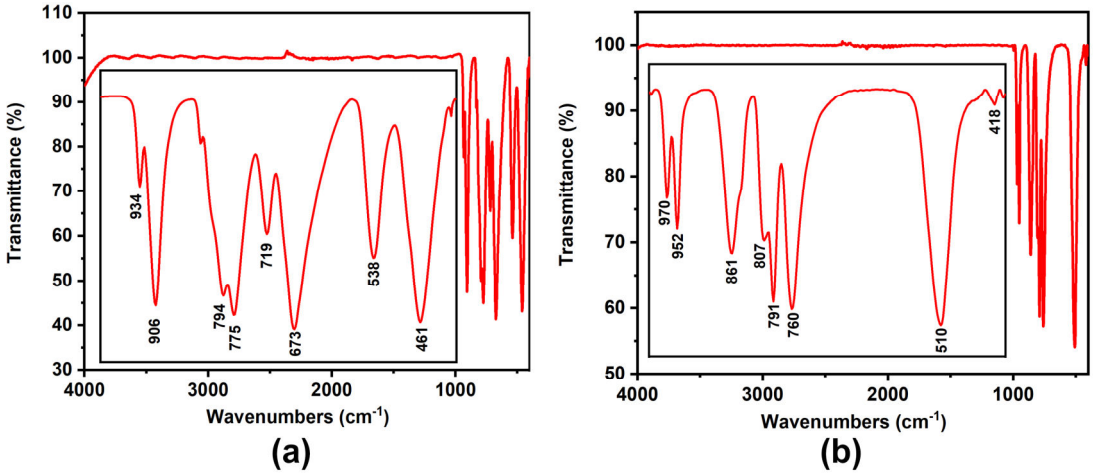

Figure S4. Infrared spectra of $Sr[VO_2F(IO_3)_2]$ (a) and $Sr_3F_2(VO_2F_4)(IO_3)$ (b).

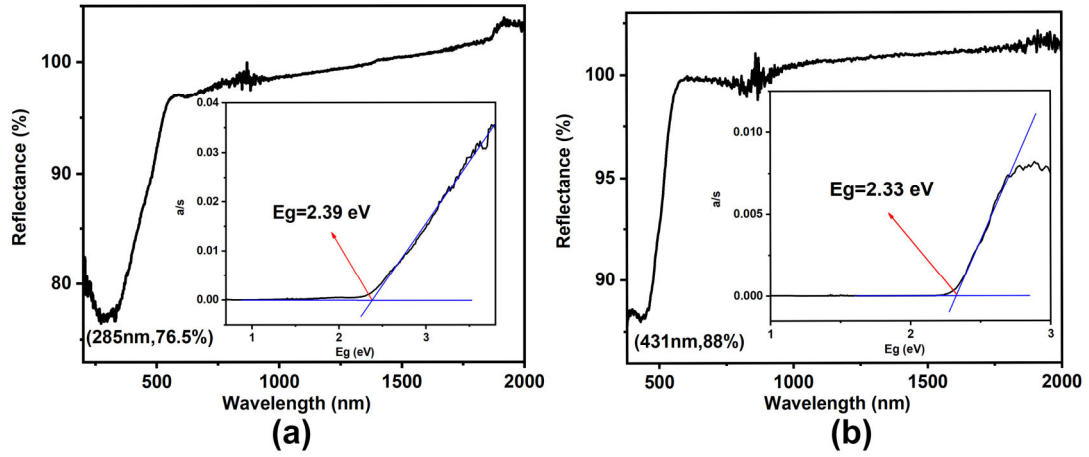

Figure S5. Ultraviolet–visible–near-infrared diffuse reflectance spectra of $Sr[VO_2F(IO_3)_2]$ (a) and $Sr_3F_2(VO_2F_4)(IO_3)$ (b).

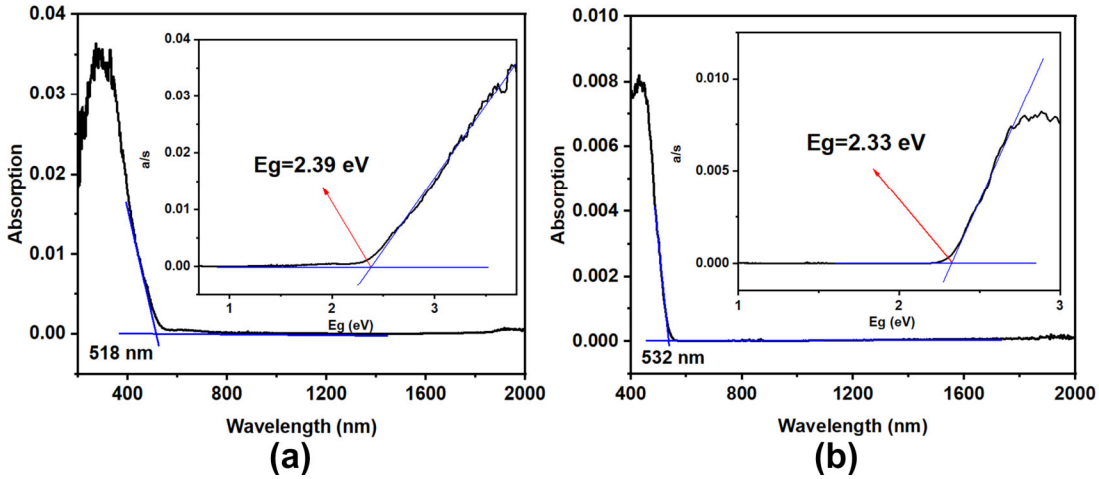

Figure S6. Ultraviolet–visible–near-infrared absorption spectra of $Sr[VO_2F(IO_3)_2]$ (a) and $Sr_3F_2(VO_2F_4)(IO_3)$ (b).

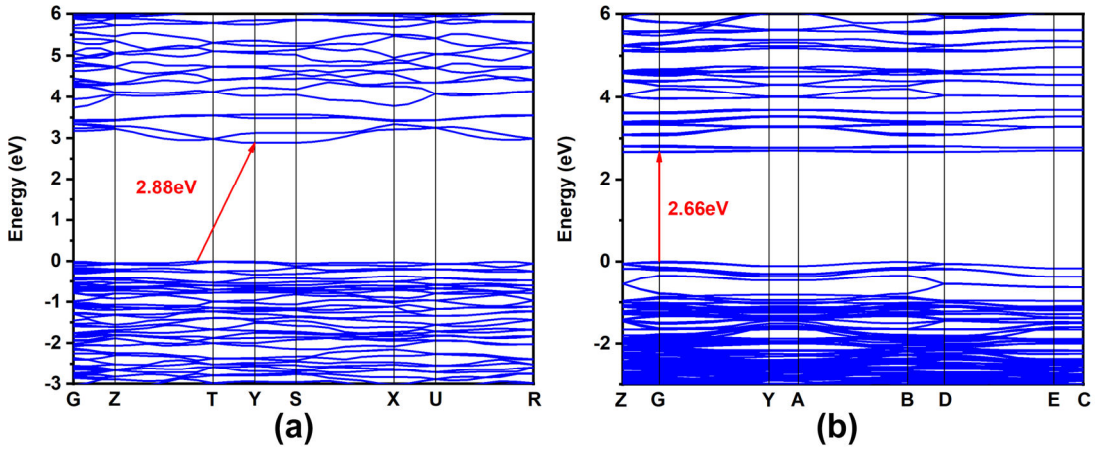

Figure S7. Calculated band structures of $Sr[VO_2F(IO_3)_2]$ (a) and $Sr_3F_2(VO_2F_4)(IO_3)$ (b).

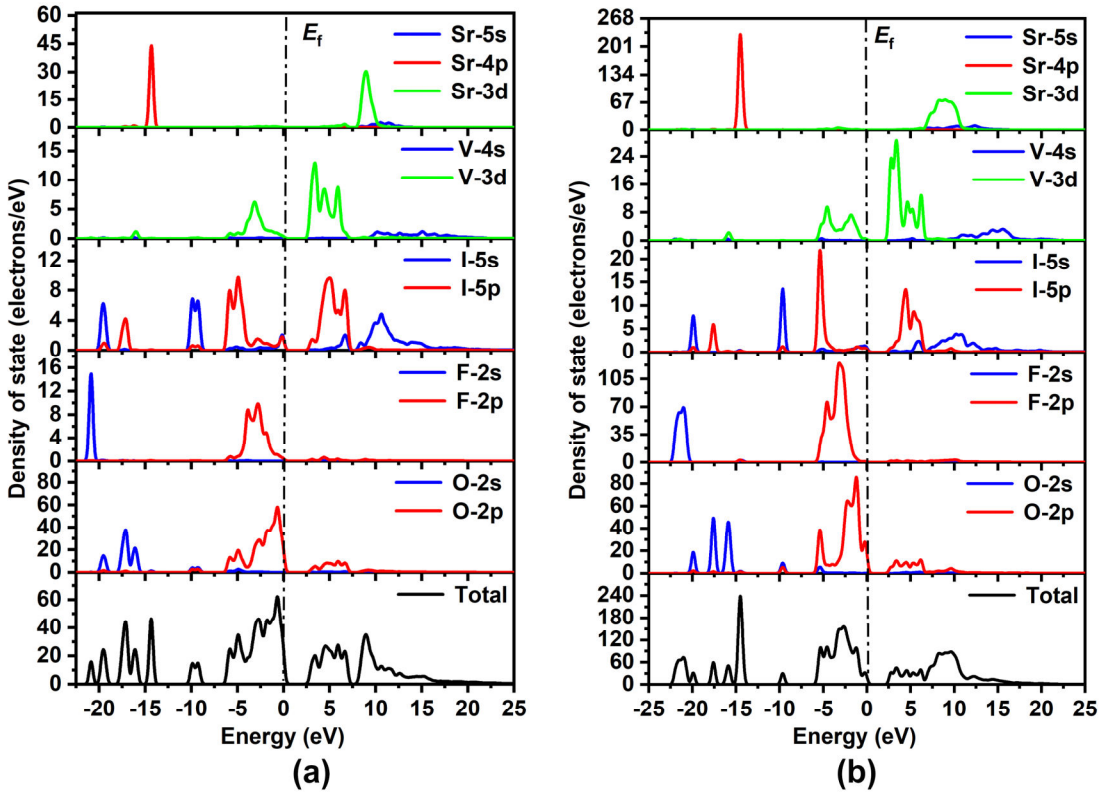

Figure S8. Partial and total density of states for $Sr[VO_2F(IO_3)_2]$ (a) and $Sr_3F_2(VO_2F_4)(IO_3)$ (b).

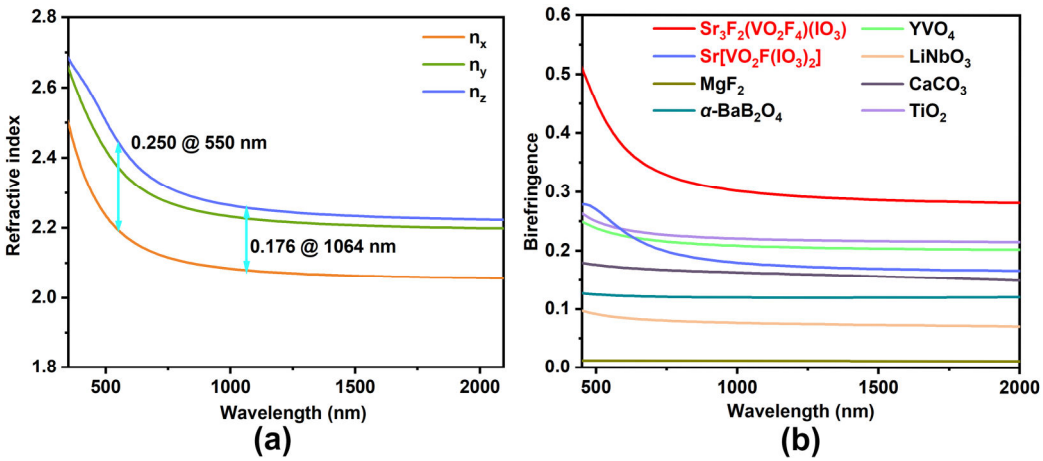

Figure S9. Calculated frequency-dependent refractive indices of $Sr[VO_2F(IO_3)_2]$ (a). Birefringences of calculated birefringences of $Sr[VO_2F(IO_3)_2]$ and $Sr_3F_2(VO_2F_4)(IO_3)$ and commercially available birefringent crystals (b).

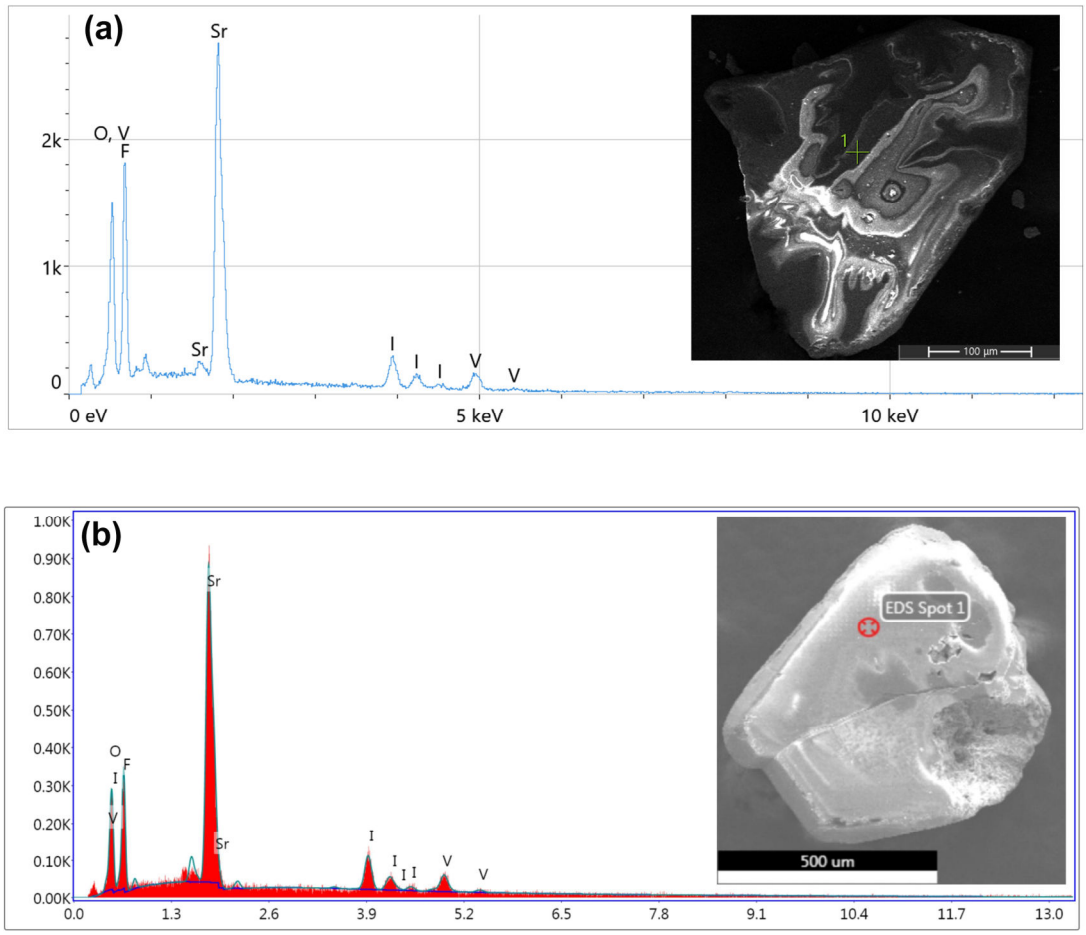

Figure S10. Energy dispersive spectroscopy analysis for $Sr[VO_2F(IO_3)_2]$ (a) and $Sr_3F_2(VO_2F_4)(IO_3)$ (b).

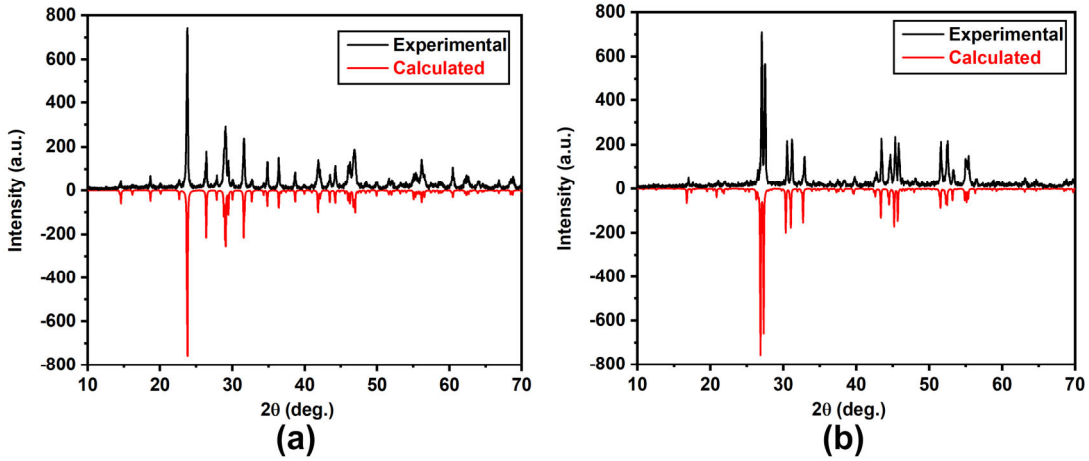

Figure S11. Simulated and experimental powder X-ray diffraction patterns of $Sr[VO_2F(IO_3)_2]$ (a) and $Sr_3F_2(VO_2F_4)(IO_3)$ (b).

References:

1. Devore, J. R. Refractive Indices of Rutile and Sphalerite. *Journal of the Optical Society of America.* **1951**, *41*, 416-419.

2. Li, W.; Wang, Y.; Lin, H.; Shah, S. I.; Huang, C. P.; Doren, D. J.; Rykov, S. A.; Chen, J. G.; Barteau, M. A. Band gap tailoring of Nd^{3+}-doped TiO_2 nanoparticles. *Appl. Phys. Lett.* **2003**, *83*, 4143-4145.

3. Zhou, G. Q.; Xu, J.; Chen, X. D.; Zhong, H. Y.; Wang, S. T.; Xu, K.; Deng, P. Z.; Gan, F. X. Growth and spectrum of a novel birefringent alpha-BaB_2O_4 crystal. *Journal of Crystal Growth.* **1998**, *191*, 517-519.

4. Dodge, M. J. Refractive properties of magnesium fluoride. *Applied Optics.* **1984**, *23*, 1980-1985.

5. Chaney, R. C. SELF-CONSISTENT ENERGY-BAND STRUCTURE OF MAGNESIUM FLUORIDE USING THE LCAO METHOD. *Journal of Physics C-Solid State Physics.* **1980**, *13*, 5691-5699.

6. Zelmon, D. E.; Small, D. L.; Jundt, D. Infrared corrected Sellmeier coefficients for congruently grown lithium niobate and 5 mol. % magnesium oxide-doped lithium niobate. *Journal of the Optical Society of America B-Optical Physics.* **1997**, *14*, 3319-3322.

7. Jia, Z.; Zhang, N. N.; Ma, Y. Y.; Zhao, L. W.; Xia, M. J.; Li, R. K. Top-Seeded Solution Growth and Optical Properties of Deep-UV Birefringent Crystal $Ba_2Ca(B_3O_6)_2$. *Crystal Growth & Design.* **2017**, *17*, 558-562.

8. Wang, N. Z.; Liang, F.; Yang, Y.; Zhang, S. Z.; Lin, Z. S. A new ultraviolet transparent hydra-cyanurate $K_2(C_3N_3O_3H)$ with strong optical anisotropy from delocalized pi-bonds. *Dalton Trans.* **2019**, *48*, 2271-2274.

9. Boyd, G. D.; Miller, R. C.; Nassau, K.; Bond, W. L.; Savage, A. $LiNbO_3$: AN EFFICIENT PHASE MATCHABLE NONLINEAR OPTICAL MATERIAL. *Appl. Phys. Lett.* **1964**, *5*, 234-236.

10. Luo, H. T.; Tkaczyk, T.; Dereniak, E. L.; Oka, K.; Sampson, R. High birefringence of the yttrium vanadate crystal in the middle wavelength infrared. *Optics Letters.* **2006**, *31*, 616-618.

11. Ghosh, G. Dispersion-equation coefficients for the refractive index and birefringence of calcite and quartz crystals. *Opt. Commun.* **1999**, *163*, 95-102.

12. Chen, Y. X.; Chen, Z. X.; Zhou, Y.; Li, Y. Q.; Liu, Y. C.; Ding, Q. R.; Chen, X.; Zhao, S. G.; Luo, J. H. An Antimony(III) Fluoride Oxalate with Large Birefringence. *Chemistry-a European Journal.* **2021**, *27*, 4557-4560.

13. Yang, B. P.; Hu, C. L.; Xu, X.; Sun, C. F.; Zhang, J. H.; Mao, J. G. $NaVO_2(IO_3)_2(H_2O)$: A Unique Layered Material Produces A Very Strong SHG Response. *Chemistry of Materials.* **2010**, *22*, 1545-1550.

14. Chen, J.; Hu, C. L.; Lin, Y. L.; Chen, Y.; Chen, Q. Q.; Mao, J. G. $K_3V_2O_3F_4(IO_3)_3$: a high-performance SHG crystal containing both five and six-coordinated V^{5+} cations. *Chem Sci.* **2022**, *13*, 454-460.

15. Chen, J.; Hu, C. L.; Zhang, X. H.; Li, B. X.; Yang, B. P.; Mao, J. G. $CsVO_2F(IO_3)$: An Excellent SHG Material Featuring an Unprecedented 3D $[VO_2F(IO_3)]^-$ Anionic Framework. *Angew Chem Int Ed Engl.* **2020**, *59*, 5381-5384.

16. Ding, M. M.; Wu, H. P.; Hu, Z. G.; Wang, J. Y.; Wu, Y. C.; Yu, H. W. $Cs_2VOF_4(IO_2F_2)$: Rationally designing a noncentrosymmetric early-transition-metal fluoroiodate. *Journal of Materials Chemistry C.* **2022**, *10*, 12197-12201.

17. Yu, H. W.; Nisbet, M. L.; Poeppelmeier, K. R. Assisting the Effective Design of Polar Iodates with Early Transition-Metal Oxide Fluoride Anions. *J Am Chem Soc.* **2018**, *140*, 8868-8876.

18. Yang, B. P.; Hu, C. L.; Xu, X.; Huang, C.; Mao, J. G. $Zn_2(VO_4)(IO_3)$: A Novel Polar Zinc(II) Vanadium(V) Iodate with a Large SHG Response. *Inorganic Chemistry.* **2013**, *52*, 5378-5384.

19. Lin, L.; Jiang, X. X.; Wu, C.; Lin, Z. S.; Huang, Z. P.; Humphrey, M. G.; Zhang, C. $CsZrF_4(IO_3)$: The First Polar Zirconium Iodate with cis-$[ZrO_2F_6]$ Polyhedra Inducing Optimized Balance of Large Band Gap and

Second Harmonic Generation. *Chemistry of Materials.* **2021**, *33*, 5555-5562.
20. Chen, X. A.; Zhang, L.; Chang, X. N.; Xue, H. P.; Zang, H. G.; Xiao, W. Q.; Song, X. M.; Yan, H. $LiMoO_3(IO_3)$: A new molybdenyl iodate based on WO_3-type sheets with large SHG response. *Journal of Alloys and Compounds.* **2007**, *428*, 54-58.
21. Chen, J.; Hu, C. L.; Li, Y. L.; Chen, Q. Q.; Li, B. X.; Mao, J. G. $AMoO_3(IO_3)$ (A = Na and K): Two promising optical materials via properly assembling the Λ-shaped basic building units. *Journal of Alloys and Compounds.* **2022**, *894*, 162547.
22. Li, Y. H.; Han, G. P.; Yu, H. W.; Li, H.; Yang, Z. H.; Pan, S. L. Two Polar Molybdenum(VI) Iodates(V) with Large Second-Harmonic Generation Responses. *Chemistry of Materials.* **2019**, *31*, 2992-3000.
23. Hu, Y. L.; Jiang, X. X.; Wu, C.; Huang, Z. P.; Lin, Z. S.; Humphrey, M. G.; Zhang, C. $A_2MoO_2F_3(IO_2F_2)$ (A = Rb, Cs): Strong Nonlinear Optical Responses and Enlarged Band Gaps through Fluorine Incorporation. *Chemistry of Materials.* **2021**, *33*, 5700-5708.
24. Hou, Y.; Wu, H. P.; Yu, H. W.; Hu, Z. G.; Wang, J. Y.; Wu, Y. C. An Effective Strategy for Designing Nonlinear Optical Crystals by Combining the Structure-directing Property of Oxyfluorides with the Chemical Substitution. *Angew Chem Int Ed Engl.* **2021**, *60*, 25302-25306.
25. Huang, Q. M.; Hu, C. L.; Yang, B. P.; Tang, R. L.; Chen, J.; Fang, Z.; Li, B. X.; Mao, J. G. $Ba_2[MoO_3(OH)(IO_3)_2]IO_3$: A Promising SHG Material Featuring a Λ-Shaped Functional Motif Achieved by Universal Mono-Site Substitution. *Chemistry of Materials.* **2020**, *32*, 6780-6787.
26. Wu, C.; Jiang, X. X.; Wang, Z. J.; Lin, L.; Lin, Z. S.; Huang, Z. P.; Long, X. F.; Humphrey, M. G.; Zhang, C. Giant Optical Anisotropy in the UV-Transparent 2D Nonlinear Optical Material $Sc(IO_3)_2(NO_3)$. *Angew Chem Int Ed Engl.* **2020**, *133*, 3506-3510.
27. Wu, C.; Wu, T. H.; Jiang, X. X.; Wang, Z. J.; Sha, H. Y.; Lin, L.; Lin, Z. S.; Huang, Z. P.; Long, X. F.; Humphrey, M. G.; et al. Large Second-Harmonic Response and Giant Birefringence of $CeF_2(SO_4)$ Induced by Highly Polarizable Polyhedra. *J Am Chem Soc.* **2021**, *143*, 4138-4142.
28. Chen, J.; Hu, C. L.; Mao, F. F.; Feng, J. H.; Mao, J. G. A Facile Route to Nonlinear Optical Materials: Three-Site Aliovalent Substitution Involving One Cation and Two Anions. *Angew Chem Int Ed Engl.* **2019**, *58*, 2098-2102.
29. Huang, Q. M.; Hu, C. L.; Yang, B. P.; Fang, Z.; Huang, Y.; Mao, J. G. $Ba_2[FeF_4(IO_3)_2]IO_3$: a promising nonlinear optical material achieved by chemical-tailoring-induced structure evolution. *Chem Commun (Camb).* **2021**, *57*, 11525-11528.
30. Gai, M. Q.; Wang, Y.; Tong, T. H.; Yang, Z. H.; Pan, S. L. $ZnIO_3F$: Zinc Iodate Fluoride with Large Birefringence and Wide Band Gap. *Inorg Chem.* **2020**, *59*, 4172-4175.
31. Cao, L. L.; Luo, M.; Lin, C. S.; Zhou, Y. Q.; Zhao, D.; Yan, T.; Ye, N. From centrosymmetric to noncentrosymmetric: intriguing structure evolution in d^{10}-transition metal iodate fluorides. *Chemical communications.* **2020**, *56*, 10734-10737.
32. Peng, G.; Yang, Y.; Yan, T.; Zhao, D.; Li, B. X.; Zhang, G.; Lin, Z. S.; Ye, N. Helix-constructed polar rare-earth iodate fluoride as a laser nonlinear optical multifunctional material. *Chemical Science.* **2020**, *11*, 7396-7400.
33. Huang, Y.; Fang, Z.; Yang, B. P.; Zhang, X. Y.; Mao, J. G. A new birefringent material, $HfF_2(IO_3)_2$, with a large birefringence and improved overall performances achieved by the integration of functional groups. *Scripta Materialia.* **2023**, *223*, 115082.
34. Chen, J.; Hu, C. L.; Mao, J. G. $LiGaF_2(IO_3)_2$: A mixed-metal gallium iodate-fluoride with large birefringence and wide band gap. *Science China Materials.* **2020**, *64*, 400-407.
35. Fan, H. X.; Peng, G.; Lin, C. S.; Chen, K. C.; Yang, S. D.; Ye, N. $Ba(IO_3)F$: An Alkaline-Earth-Metal

Iodate Fluoride Crystal with Large Band Gap and Birefringence. *Inorg Chem.* **2020**, *59*, 7376-7379.
36. Wu, T.; Jiang, X.; Wu, C.; Sha, H.; Wang, Z.; Lin, Z.; Huang, Z.; Long, X.; Humphrey, M. G.; Zhang, C. From $Ce(IO_3)_4$ to $CeF_2(IO_3)_2$: fluorinated homovalent substitution simultaneously enhances SHG response and bandgap for mid-infrared nonlinear optics. *Journal of Materials Chemistry C.* **2021**, *9*, 8987-8993.
37. Abudouwufu, T.; Zhang, M.; Cheng, S. C.; Yang, Z. H.; Pan, S. L. $Ce(IO_3)_2F_2H_2O$: The First Rare-Earth-Metal Iodate Fluoride with Large Second Harmonic Generation Response. *Chemistry.* **2019**, *25*, 1221-1226.
38. Fan, H.; Lin, C.; Chen, K.; Peng, G.; Li, B.; Zhang, G.; Long, X.; Ye, N. $(NH_4)Bi_2(IO_3)_3F_5$: An Unusual Ammonium-containing Metal Iodate Fluoride Showing Strong Second Harmonic Generation (SHG) Response and Thermochromic Behavior. *Angew Chem Int Ed Engl.* **2019**, *59*, 5268 –5272.
39. Ma, N.; Huang, Y.; Hu, C. L.; Zhang, M. Z.; Li, B. X.; Mao, J. G. $Ce(IO_3)_3F$ and $Ce(IO_3)_2(NO_3)$: Two Mixed-Anion Cerium Iodates with Good Nonlinear Optical and Birefringent Properties. *Inorganic Chemistry.* **2023**, *62*, 15329-15333.
40. Yang, S. X.; Wu, H. P.; Hu, Z. G.; Wang, J. Y.; Wu, Y. C.; Yu, H. W. From $NaGa(IO_3)_3F$ to $NaGa(IO_3)_2F_2$ and $NaGa(IO_3)_4$: The Effects of Chemical Substitution between F^- Anions and IO_3^- Groups on the Structures and Properties of Gallium Iodates. *Inorganic Chemistry.* **2024**, *63*, 1404-1413.
41. Huang, Y.; Li, B. X.; Hu, C. L.; Yang, B. P.; Mao, J. G. $CsHfF_4(IO_3)$: A Hafnium Iodate Exhibiting a Strong Second- Harmonic-Generation Effect and a Wide Band Gap Achieved by Mixed-Ligand Acentric Coordination. *Inorganic Chemistry.* **2023**, *62*, 3343−3348
42. Jiang, X. Q.; Wu, H. P.; Yu, H. W.; Hu, Z. G.; Wang, J. Y.; Wu, Y. C. Synthesis, Structure, Characterization, and Calculation of a Noncentrosymmetric Fluorine-Containing Indium Iodate, $BaInF_3(IO_3)_2$. *Crystal Growth & Design.* **2021**, *21*, 4005-4012.
43. Xu, Y. Y.; Lin, C. S.; Zhao, D.; Li, B. X.; Cao, L. L.; Ye, N.; Luo, M. Chemical substitution – oriented design of a new polar $PbFIO_3$ achieving a balance between large second-harmonic generation response and wide band gap. *Scripta Materialia.* **2022**, *208*, 114347.
44. Chen, J.; Du, K. Z. $ZrF_2(IO_3)_2$ and $RbGaF_3(IO_3)$: Two Promising Birefringent Crystals Featuring 1D Metal-Fluoride Cationic Chains and Wide Bandgaps. *Inorganic Chemistry.* **2022**, *61*, 17893-17901.
45. Tang, C. C.; Jiang, X. X.; Guo, S.; Guo, R. X.; Liu, L. J.; Xia, M. J.; Huang, Q.; Lin, Z. S.; Wang, X. Y. Synthesis, Crystal Structure, and Optical Properties of the First Alkali Metal Rare-Earth Iodate Fluoride: $Li_2Ce(IO_3)_4F_2$. *Crystal Growth & Design.* **2020**, *20*, 2135-2140.
46. Cao, L. L.; Zhang, S. Z.; Zhao, D.; Li, B. X.; Yan, T.; Yang, G. S.; Lin, Z. S.; Luo, M.; Ye, N. $Cd_3(IO_3)(IO_4)F_2{\cdot}0.1CdO$: A Nonlinear-Optical Crystal with the Introduction of Fluoride into Iodate Containing Both $IO_3^-$and IO_4^{3-}Groups. *Inorganic Chemistry.* **2021**, *60*, 6040-6046.